

## **“LIULIN-ISS-2” SYSTEM FOR COSMONAUTES’ DOSIMETRIC CONTROL IN THE ISS RADIATION ENVIRONMENT**

**Tsvetan Dachev<sup>1</sup>, Borislav Tomov<sup>1</sup>, Yuri Matviichuk<sup>1</sup>,  
Plamen Dimitrov<sup>1</sup>, Vyiacheslav Shurshakov<sup>2</sup>, Victor Benghin<sup>2</sup>,  
Elena Yarmanova<sup>2</sup>, Olga Ivanova<sup>2</sup>, Igor Nikolaev<sup>3</sup>**

<sup>1</sup>Space Research and Technology Institute – Bulgarian Academy of Sciences

<sup>2</sup>Institute of Biomedical Problems – Russian Academy of Science

<sup>3</sup>S.P. Korolev Rocket and Space Corporation “Energia”, Russia  
e-mail: tdachev@bas.bg

### **Abstract**

*Under a collaboration agreement between Space Research and Technology Institute, Bulgarian Academy of Sciences (SRTI–BAS), Institute of Biomedical Problems, Russian Academy of Sciences (IBP–RAS) and S.P. Korolev Rocket and Space Corporation “Energia” an engineering model of new system named “Liulin-ISS-2”, for personal dosimetric control of Russian cosmonauts inside and outside ISS, was developed. It is expected that the new system will replace the Liulin-ISS system, launched to ISS in September 2005. The “Liulin-ISS-2” priority is focused on the active measurement with 10 seconds resolution of the dose rate dynamics from Galactic Cosmic Rays (GCR), protons from internal and energetic electrons from external radiation belts, and solar energetic particles (SEP) inside ISS modules and during the extravehicular activity (EVA) of Russian and international cosmonauts. The significance of dose measurements for EVA was formulized during the analysis of the large and rapid variations in space and time of the doses obtained simultaneously at two different locations outside the ISS [1]. Liulin-ISS-2 system consists of 4 portable dosimeters (PD) and interface block (IB) with internal dosimeter. The PD sized 66×56×26 mm is based on the traditional Liulin type DES block diagram with 2 cm<sup>2</sup> square and 0.3 mm depth PIN diode. The analysis of the obtained deposited energy spectra will be performed according the ideas for intelligent crew personal dosimeter [3] and the new experience obtained during the data analysis from the R3DR2 instrument outside ISS in the period October 2014–January 2016. A SAFT prismatic lithium-Ion rechargeable battery, endorsed for space use, is used in the PD and allows more than 7 days independent work of the PD with 10 sec resolution. Thermostat and manageable heater are implemented to keep the temperature of the PIN diode not lower than -20 °C during EVA when is situated in the cosmonauts’ spacesuit pocket. The PD can work independently on ID by using USB connection and special software with any other PC. The interface block (size 265×178×85 mm) is based on a Getac T800 (<http://www.getac.com/>) fully rugged tablet PC in compliance with the requirements and procedures of MIL-STD-810G, and under Windows-8 operational system. Through eight-port industrial USB hub the tablet PC manages the system and data transfer toward CAN serial interface and/or flash memory stick. Continuously the last 90 minutes of data, obtained with the internal dosimeter, are visualized on the screen of the tablet PC. These data can be used by the cosmonauts and the radiation control personal for fast analysis of the radiation risk for astronauts during solar proton events.*

## **1. Introduction**

### ***1.1. Purpose of “Liulin-ISS-2” instrument***

The purpose of performing the development of the “Liulin-ISS-2” is the creation of dosimetric equipment for operational individual monitoring of the crew aboard the Russian segment of the International Space Station (ISS), both in the compartments and outside the ISS. Dosimeter "Liulin-ISS-2" priority is focused on the active measurement of dose rate dynamics with 10 s resolution of the energetic protons and electrons from internal and outer Earth's Radiation Belts (RB) during ExtraVehicular Activity (EVA) in the cosmonauts' space suit pocket. Similar measurements on the ISS have not been carried out yet.

According to the results of measurements that were carried out previously on the external surface of the ISS with two devices R3DE/R [1] – they are similar to dosimeter "Liulin-ISS-2" described in this article – it was concluded the possibility of large (more than an order of magnitude) and rapid (within ~ 10 s) dose rate variations caused by different shielding of the detectors and anisotropy of the radiation sources.

The R3DE/R instruments' results can be interpreted as the possible doses received by astronauts and cosmonauts during EVA, because the shielding of the R3DE/R detectors is close to the value of shielding of the space suits of the Russian and American cosmonauts and astronauts [2]. Tooling solution was proposed in [3], where on the basis of analysis of the shape of the energy spectrum and the relationship of dose to the flux (specific dose), is feasible in principle to distinguish between the predominant sources of cosmic radiation on the ISS orbit and calculate the equivalent dose for them. These ideas were confirmed during the latest experiment on ISS with the R3DR2 instrument in the period October 2014–January 2016 [4]. The dosimeter "Liulin-ISS-2" will apply the basic instrument and software developments, which were made in the papers [4, 5].

### ***1.2. Analysis of the research object and the state of the art***

Cosmic radiation is an unavoidable factor in spaceflight, which it is impossible to eliminate, due to restrictions on weight, power consumption and other spacecraft resources. In connection with the proposed future expansion of space activities (missions to asteroids and to the Moon, interplanetary manned missions, etc..) and, as a consequence, an increase in terms of human presence on board the spacecraft importance of this factor will steadily increase. At the present time the usual stay of astronauts on the ISS is months-long, as well as holding a number of flights during the career. In addition, there are plans in the near future to carry out a manned mission to Mars, which implies a long-term stay of the person in space.

The essential point in the planning and development of long-term space flight is the impact of radiation on the crew [6–8], the dose received by an astronaut in a space flight, associated with the effect of various radiation sources.

### ***1.2.1. Galactic Cosmic Ray (GCR)***

A Galactic Cosmic Ray (GCR) consists of protons and heavy nuclei – practically the entire periodic table of elements of D.I. Mendeleev. The GCR particles are accelerated in the depths of space to energies at which the particles penetrate through casing spacecraft, creating at the same time in the nuclear reactions secondary charged particles and neutrons.

The amplitude changes of GCR intensity during solar cycle phase for different energies is different. For example, for  $E_p \sim 100 \sim \text{MeV}$  it reaches 100 %, whereas for  $E_p \geq 2 \div 3 \text{ GeV}$  its magnitude does not exceed 1  $\div$  2 %. Integral flow GCR ( $10^6 \div 10^{21} \text{ eV}$ ) in interplanetary space is changed under the influence of solar modulation, and near the Earth's orbit is  $J(\text{GCR}) = 2 \div 4.5 \text{ cm}^{-2} \text{ s}^{-1}$ , the minimum GCR flux value is realized in the period of the SA maximum, and the maximum - in minimum period.

In the near-Earth space, due to the shielding effect of the Earth GCR flux, decreases 2 times, and even additional attenuation GCR flux occurs due to the conditions of entry into the geomagnetic field. The flow of GCR particles in Earth orbit outside the magnetosphere with a high degree of accuracy can be considered isotropic.

In terms of dynamic performance, the FCL can be attributed to sources of chronic exposure of biological objects. GCR dose rate inside the ISS at altitude of 400 km and inclination  $51.6^\circ$  can be estimated as  $100 \div 200 \mu\text{Gy day}^{-1}$ . Due to the hard spectrum absorbed dose of the GCR varies slightly with the thickness of the protection.

### ***1.2.2. Inner Radiation Belt (IRB)***

High-energy charged particles are trapped by the Earth's magnetic field and form two distinct belts of toroidal shapes surrounding the Earth. These are called radiation belts (RB). The IRB is situated at an altitude of 0.2  $\div$  2.0 Earth radii and consists of both electrons, with energies of up to 10 MeV, and protons with energies of up to 700 MeV. Outside of the ISS, the IRB energetic protons delivered the highest daily dose rates.

During an analysis of the R3DE and R3DR data, it was discovered that the US space shuttle dockings with ISS decreased the IRB dose rate delivered by IRB 30  $\div$  150 MeV proton fluxes [9]. The effect was attributed to the additional shielding provided by the 78-ton shuttle.

### ***1.2.3. Outer Radiation Belt (ORB)***

The Outer Radiation Belt (ORB) is located in the altitudinal range of 3.4÷10 Earth radii. The ORB population is electrons with energies  $> 10$  MeV. The first observations of the ORB relativistic electron fluxes in the ISS were made in 2001 with a Liulin-E094 instrument (Dachev et al., 2002a; Reitz et al., 2005) inside the US laboratory module. The effects of the relatively small ORB dose rates were not fully understood in 2002. ORB relativistic electron fluxes were observed with Liulin DES type instruments flown on ISS and LEO satellites [10–12]. The ORB daily dose rate was practically zero on magnetic quiet days, but reached maximum dose rates up to  $288.40 \mu\text{Gy h}^{-1}$  in the disturbed periods after magnetic storms.

### ***1.2.3. Solar Energetic Particles (SEP)***

Solar flares, caused by sporadic eruptions in the chromosphere and corona of the Sun, produced high fluxes of charged solar energetic particles (SEP) with energies up to several GeV. We measured the characteristics of SEP from September till October 1989 inside the Russian space station “MIR” with the first Liulin type instrument [13] and with the Liulin-5 dosimetric telescope (DT) inside the ISS in March 2012 [14]. With the R3DR2 instrument, we performed one of the first SEP measurements outside of the ISS [15]. The highest SEP hourly dose rate measured during the EXPOSE-R2 mission was  $5251 \mu\text{Gy h}^{-1}$  on June 22, 2015. Historically the SEP measurements inside the ISS are rare, but have been discussed in [16, 17].

## **2. Instrumentation**

The engineering model of the “Liulin-ISS-2” instrument consists of three units: 2 portable dosimeters (PD) and 1 interface block (IB) with one stationary dosimeter inside (Fig. 1).



*Fig. 1. External view of “Liulin-ISS-2” instrument*

### ***2.1. “Liulin-ISS-2” interface block (IB) description***

The interface block (IB) is situated in a black painted aluminum box sized 265×178×85 mm with weight of about 3 kg. On the upper panel of the IB is seen the Getac-T800 type (URL: <http://www.getac.com/>) fully rugged tablet personal computer (PC). There are 3 LED indicators and 6 buttons seen on the right side of the IB, which serve the PC management. The touch screen of the PC is foreseen to be switched OFF in the most of the time in space. The cosmonaut may see the information on the screen after simple touch of it.

Two portable dosimeters are seen connected with USB cables to the IB. The two more USB cable, which may be seen on Fig. 1, are foreseen for the extension of the engineering model up to a system with 4 portable dosimeters.

On the right panel of the IB (Fig. 2.) are mounted from left to right as follows: the ground bolt; the 7-pin 28 V power connector; the 10-pin Controller Area Network (CAN) interface connector; the Universal Serial Bus (USB) connector for flash memory stick connection; 2 fuses; the 28 V power ON/OFF switch and the green Light Emitting Diode (LED), which indicate when the power switch is in position ON. (All labels on the engineering model are preliminary. During the final development of it, these labels will be replaced with better made permanent labels.)



*Fig. 2. External view of the right panel of the IB*

The whole “Liulin-ISS-2” system and IB are managed by the Getac-T800 type tablet PC in compliance with the requirements and procedures of MIL-STD-810G, and under Windows-8 operational system (OS). Except the PC in the IB are situated the following blocks: DC/DC converter from 22÷32 V to 19 V, which supplies with power the tablet PC; 4 DC/DC converters from 8.4 V to 5 V, which powered the PD and charged their batteries; 8-port USB hub, which communicate upstream with the tablet PC and with 7 downstream USB devices as follows: 4 PD, 1 internal dosimeter (ID), 1 USB-controller area network (CAN) bus module, and 1 USB flash drive (Fig. 3).

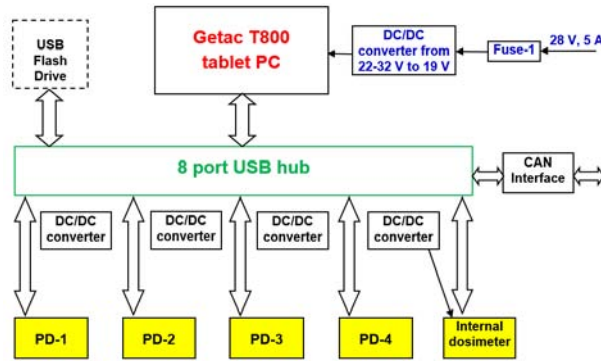


Fig. 3. Block-diagram of “Liulin-ISS-2” instrument

## 2.2. Description of “Liulin-ISS-2” dosimeters

The design of the internal and portable dosimeters-spectrometers of the engineering model of “Liulin-ISS-2” instrument is not new. Recently published paper by [18] includes list and description of all the experiments carried out with the participation of SRTI-BAS for measuring cosmic radiation from 1988 to August 2014 using dosimeters similar to these in “Liulin-ISS-2” on satellite, rocket, balloons, and aircraft.

The external view of the portable dosimeters is seen in Fig. 4a. It is situated in an oxidised aluminium box with size 66×56×26 mm and weight of 0.135 kg. Below the upper panel of PD (Fig. 4b) are mounted the ON/OFF switch, the red status LED, and the USB mini female connector. Below the panel is situated the space qualified SAFT rechargeable lithium-ion battery MP 144350 type. It is foreseen an opportunity for change of the battery by removing of the upper panel by unscrewing the 2 bolts.

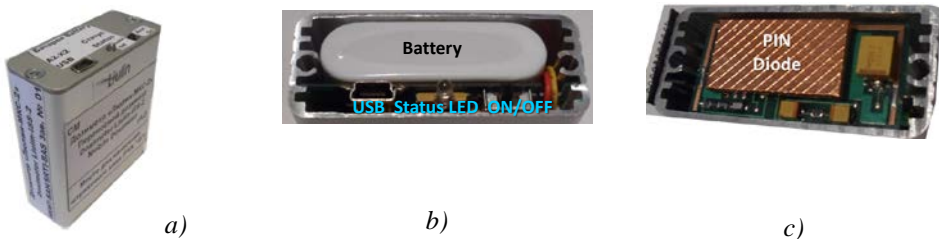


Fig. 4: a) External view of the “Liulin-ISS-2” PD, b) view below upper panel of PD, c) view below lower panel of PD

Below the 0.5 mm thick bottom panel of PD (Fig. 4c) is situated the 2 cm<sup>2</sup> PIN diode detector. In addition, there is a technological shielding of 0.07 mm copper and 0.2 mm plastic material, which provide total shielding of 0.25 g cm<sup>-2</sup>. The calculated required kinetic energies of normally falling particles to the detector are 0.67 and 12.5 MeV for electrons and protons, respectively (URL: <https://www.nist.gov/pml/stopping-power-range-tables-electrons-protons-and-helium-ions>). This indicates that only protons and electrons with energies higher than the values listed above can cross the PD shielding materials and reach the surface of the detector.

The “Liulin-ISS-2” portable dosimeters and the IB internal dosimeter are Liulin type deposited energy spectrometers (DES), which use one silicon detector to measure the deposited energy and number of particles that allow calculating the dose rate and particle flux.

On Fig. 5 is presented the block diagram of the engineering model of “Liulin-ISS-2” portable dosimeters. The internal dosimeter contains only some of the blocks: semiconductor detector, charge-sensitive preamplifier, a fast 256 bits analogue-to-digital converter (ADC), discriminator, and 2 microcontrollers. It is managed directly by the PC through the USB port and its deposited energy spectra are stored in the PC also.

The PD consists of all blocks seen in Fig. 5 but are managed only by one microcontroller. Except the mentioned, in the internal dosimeter blocks, they consist of: 2 MB flash memory to store the spectra, clock-calendar, battery charge controller, and SAFT rechargeable battery. Thermostat and manageable heater are implemented to keep the temperature of the PIN diode detector not smaller than -20 °C during EVA when is situated in the cosmonauts’ spacesuit pocket.

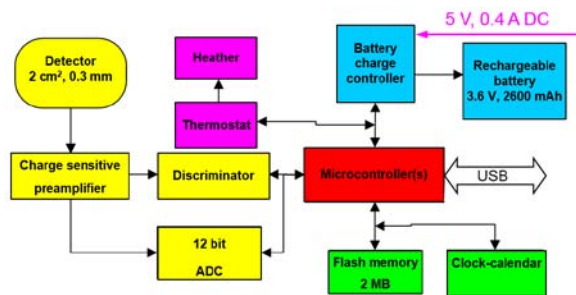


Fig. 5. Block-diagram of “Liulin-ISS-2” dosimeters

### 3. Dose determination

Pulse analysis technique is used to obtain the deposited energy from each photon/particle crossing partially or fully the silicon detector of the dosimeters. The deposited energies organised in 256 channels form the deposited energy spectrum

for each measurement cycle. It is further used for the calculation of the absorbed dose and flux in the silicon detector from primary and secondary particles. The analysis of the shape of the spectrum and the dose to flux ratio, known also as specific dose (SD), permits the characterization of the predominant radiation source in the DES environment [19].

The internal and external dosimeters are managed by the microcontrollers through specially developed firmware. The ADC and the microcontroller measure organize and keep in RAM memory the 256 channels deposited energy spectra. The microcontroller(s) manages the whole work of the dosimeters and data outputs toward the USB connection.

The main measured parameter in the dosimeters is the amplitude of the pulse after the charge-sensitive preamplifier, generated by a particle or a photon crossing partially or fully the detector. The amplitude of the pulse is proportional by a factor of  $240 \text{ mV MeV}^{-1}$  to the energy deposited in the detector and to the dose, respectively. By 12 bit ADC these amplitudes are digitized and organized in a 256-channel deposited energy spectrum.

By definition the dose in the silicon detector  $D_{Si}$  [Gy] is one Joule deposited in 1 kg of matter. The dosimeters absorbed dose is calculated by dividing the summarized energy deposition in the spectrum in Joules to the mass of the detector in kilograms [20]:

$$(1) \quad D_{Si} [\text{Gy}] = K \sum_{i=1}^{255} (EL_i) [J] / MD [\text{kg}]$$

where  $K$  is a coefficient,  $MD$  is the mass of the detector, and  $EL_i$  is the energy loss in Joules in the channel  $i$ . The energy in MeV is proportional to the amplitude  $A$  of the pulse:  $EL_i [\text{MeV}] = A [\text{V}] / 0.24 [\text{V/MeV}]$ , where  $0.24 [\text{V/MeV}]$  is a coefficient dependent on the preamplifier used and its sensitivity.

All 255 deposited dose values, depending on the deposited energy for one exposure time, form the deposited energy spectrum. The energy channel number 256 accumulates all pulses with amplitudes higher than the upper energy of 20.83 MeV measured by the spectrometer.

On Fig. 6 are shown deposited energy spectra from different calibrations of the DES, which are compared with experimental proton, electron and GCR spectra obtained at aircraft altitudes and spacecraft orbit. The individual spectra seen in the figure are obtained after averaging various numbers of primary spectra and are plotted in coordinates as deposited energy per channel/deposited per channel dose rate. This allows for a better understanding of the process of formation of the spectra in different deposited energy ranges. According to Eq. (1) the absorbed dose in Si is the area between the curve of the deposited energy spectrum and the abscissa. That is why from bottom to top each spectra position against the ordinate



axes depends on the value of the deposited dose rates in Si seen in the legend at the top of the figure. The higher the measured dose rate, the higher the position of the spectrum against the ordinate axis, and the greater the area between the spectrum and the abscissa. The lowest line spectrum in Fig. 6 was obtained by Prof. Frantisek Spurny during the calibration of the Liulin-4C Mobile Dosimetry Unit MDU#2, with  $^{60}\text{Co}$  as a reference radiation source, at the Nuclear Physics Institute of the Czech Academy of Sciences [19a]. This spectrum is the shortest because the energy of the  $^{60}\text{Co}$  gamma emission line is 1.2 MeV. The absolute values of the dose rates obtained from the spectra are in very good agreement with the dose rates calculated using the EGS4 transport code (URL: <http://rcwww.kek.jp/research/egs/>). The values of the measured doses were found to be within 2.8% of the reference value for the  $^{137}\text{Cs}$  source and within 8 % of the  $^{60}\text{Co}$  source [19a]. The calibrations showed that the DES had high effectiveness with respect to gamma rays, which allowed monitoring of the natural background radiation.

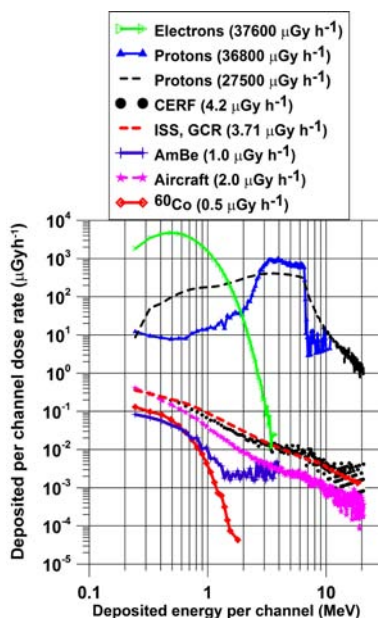


Fig. 6. Different spectral shapes obtained by Liulin-type instruments during calibrations on aircraft and spacecraft

The spectrum denoted by crosses in Fig. 6 was generated by a reference AmBe radiation source emitting neutrons with an average energy of 4.4 MeV. This spectrum continues up to about 4 MeV deposited energy with an obvious change in the slope around 1.2 MeV deposited energy. The neutron sensitivity of the DES

was further studied in the CERN-EU high-energy reference field (CERF) facility, on aircraft and in the near Earth radiation environment.

The spectrum with heavy dots in Fig. 6, obtained in the CERF facility field, contains events in all channels of the DES including the 256<sup>th</sup> channel, devoted to energy depositions above the upper level of the spectrometer at 20.83 MeV. The events seen below 1 MeV in AmBe and at CERF represent the contribution of low LET radiation (electrons, muons, etc.), while the events above 1 MeV represent the high LET components (protons, neutrons and ions heavier than H<sup>+</sup>). This idea was further developed and allowed calculation of the ambient dose equivalent  $H^*(10)$  at aircraft altitudes from the deposited energy spectrum in the Si-detector [21–23].

The CERF energy deposition spectrum is very similar to the averaged aircraft spectrum shown with asterisks in Fig. 6. This spectrum is obtained by averaging Czech Airlines aircraft data during mean solar activity at altitudes close to 10.6 km on routes between Prague and the North American cities New York and Montreal [24]. The ISS R3DE instrument mean GCR deposited energy spectrum (heavy dashed line) has a shape even closer to the CERF spectrum.

Due to the proximity of the spectra in CERF, at the aircraft altitude and at ISS (See the bunch of 3 spectra in the middle of Fig. 6) and using the idea for the 2 parts of spectra, it is possible to be calculated the different sources ambient dose equivalent rate in the dosimeters of the "Liulin-ISS-2" engineering model with the following formulas:

$$(2) \quad H^*(10)_{GCR}[Sv] = \left\{ \sum_{i=1}^{15} (EL_i)[J] / MD[kg] + 5 \sum_{i=16}^{256} (EL_i)[J] / MD[kg] \right\}$$

$$(3) \quad H^*(10)_{IRB}[Sv] = \left\{ \sum_{i=1}^{15} (EL_i)[J] / MD[kg] + 1.3 \sum_{i=16}^{256} (EL_i)[J] / MD[kg] \right\}$$

$$(4) \quad H^*(10)_{ORB}[Sv] = \left\{ \sum_{i=1}^{15} (EL_i)[J] / MD[kg] + \sum_{i=16}^{256} (EL_i)[J] / MD[kg] \right\}$$

We suppose that: the average quality factor of GCR is 5, the IRB protons average quality factor is 1.3 and the energetic electrons in the ORB is 1.

The CERF, ISS and aircraft spectra in Fig. 6 show a similar knee around 6.5÷7 MeV deposited energy. To explain the knee in Fig. 6 a spectrum with heavy triangles was added to the figure. This was obtained during calibrations of DES (non-shielded detector) with a 7.8 MeV protons beam at the cyclotron facility of the University of Louvain, Belgium. The knee seen at about 6.3 MeV corresponds to the point where the incident energy of the normally incident beam on a 0.3 mm thick detector is equal to the deposited energy. All normally incident protons with energies less than 6.3 MeV are stopped in the detector.

The light-dashed spectrum in Fig. 6 was obtained by the RADOM instrument on the Chandrayaan-1 satellite by averaging of 60 primary 10-s resolution spectra. This spectrum shows a very similar shape to the cyclotron

facility spectrum (full triangle spectrum) and a knee at the same position. This is because the energy of the inner belt protons falling on the detector is calculated to be 7÷8 MeV, i.e. equal to the energy of the cyclotron facility's monoenergetic protons falling on the non-shielded detector.

The green open triangle spectrum is the highest one in Fig. 6. It was obtained on the Chandrayaan-1 satellite at altitudes of the ORB (22000 km). This spectrum with a predominant electron population is the result of averaging 120 spectra with 10-s resolution. Only the part with deposited energies up to 4.0 MeV is shown.

The DES effectiveness for neutrons depends on their energy, being minimal for neutrons with energy of 0.5 MeV and having a maximum of a few percent for neutrons with energies of 50 MeV in the CERN field [21]. According to the "neutron induced nuclear counter effect" introduced for the Hamamatsu PIN diodes of type S2744-08 [25] almost all DESs used the same type PIN diodes and neutrons could be observed in all channels of the spectrum with a probability at least one order of magnitude higher in the first 15 channels.

#### 4. Radiation source separation example

It is expected that, on ground after the EVA experiments on ISS, using the formulas (1–4) we will be able to separate and analyze the variations of four different radiation sources dose rates obtained by the PD. The current section aims to confirm this and to present the expected values on ISS radiation sources. The methods for sources separation in the internal dosimeter is described in the next section of the article.

The following four primary radiation sources were expected and recognized in the data obtained with the R3DR2 instrument on ISS in the period 24.10.2014–11.01.2016: (i) globally distributed GCR particles and those derived from them; (ii) protons in the SAA region of the IRB; (iii) relativistic electrons and/or *bremsstrahlung* in the high latitudes of the ISS orbit where the ORB is situated; and (iv) solar energetic particles (SEP) in the high latitudes of the ISS orbit. Together with the real SEP particles, a low flux of what were likely to be mostly secondary protons (SP), were observed in the data.

The simplest method for source separation is described by [19]. It is based on the Heffner formulae [26]; The Heffner's formulae were recently published by [19] and shows that the data can be simply split into two parts by using the dose to flux ratio (D/F) or specific dose (SD). When the SD is less than  $1.12 \text{ nGy cm}^2 \text{ particle}^{-1}$ , the expected predominant type of radiation in a 10 s interval is ORB electrons. When the SD is greater than  $1.12 \text{ nGy cm}^2 \text{ particle}^{-1}$ , the expected type of radiation is IRB or SEP protons. The GCR source is divided between the two ranges.

The separation statistics of the R3DR2 data show the following results [5]: 441 days were covered; 3,810,240 points were separated; 2398 were lost (0.062 %) or on average less than 6 points per day; and 313 points were counted twice. The average source counts per day were as follows: GCR 7636 points, IRB 573 points, ORB 383 points, SEP counts per 27 days were 148 points; average, SP counts per 414 days (days without real SEP) were 34 points. The number of daily-averaged measurements for the “stable” presented sources are: 7636+573+383+34, or 8626 measurements in total, which were selected from a total of 8640.

In Fig. 7 in 4 panels is represented the end result of the division of 4 radiation sources and their variations for the period October 24, 2014–January 11, 2016 (Preliminary data were published in [4, 5, 27]).

The GCR source average daily doses variations are presented with a thick black line in Fig. 3a. At the top of this panel with red line is shown the variation of *Dst* (Disturbance Storm Time) index (URL: <http://wdc.kugi.kyoto-u.ac.jp/index.html>), which for the days after the beginning of the magnetic storms have negative values, reaching -223 nanoteslas on March 17 and -204 nanoteslas on June 23<sup>rd</sup>. Well defined correlation between daily-average dose and *Dst* index confirmed a phenomenon of reduction the flux of GCR particles during the main phase of the magnetic storm, known by the term “Forbush decreases”.

A very small almost linear trend of increase was observed in the data for average daily doses of GCR. The minimum value of  $\sim 72 \mu\text{Gy d}^{-1}$  was at the beginning of observations in October 2014 and maximum values of  $73 \mu\text{Gy d}^{-1}$  was at the end of observations through January 2016. The reason is declining solar activity during the period of observation.

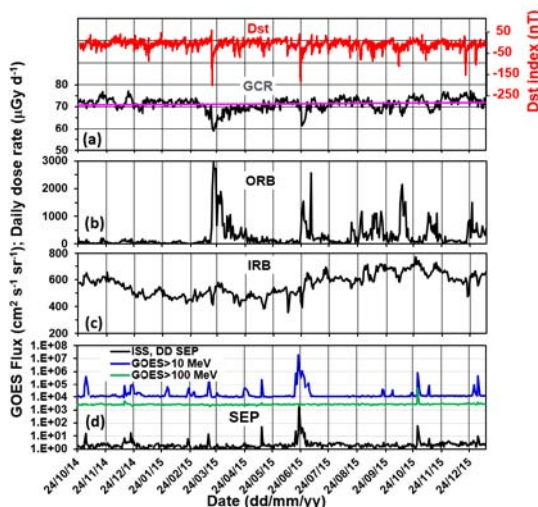


Fig. 7. Radiation sources dynamics as observed on ISS by R3DR2 instrument in the period November 2014–January 2016

The variations in average daily doses of relativistic electrons in ORB are shown in Fig. 3b. Clearly visible are 2 periods in the data. In relatively “quiet” period of geomagnetic activity, between 24 October 2014 and mid-March 2015 the values of average daily doses of relativistic electrons in ORB were relatively small and ranged  $2\div 200 \mu\text{Gy d}^{-1}$ . In the second period, between mid-March 2015 and the end of observations the fluctuations in average daily doses in ORB are larger and reached values up to about  $3000 \mu\text{Gy d}^{-1}$ , being in anti-correlation with *Dst* index (red line) in the top panel of Fig. 7. This was in result of the acceleration of electrons and filling the ORB with them.

The next relatively “stable” source of doses outside the ISS was the energy protons in IRB, which are shown by a thick black line in Fig. 3c. The main reason for the long time variation was the correlation with the average altitude of the station above the Earth. Higher doses at the end of the mission are also associated with a lower solar activity, which results in small concentrations in the neutral atmosphere of the earth and respectively to smaller losses from recombination of energetic protons in the IRB.

In Fig. 7d are presented the variations in the average daily dose of SEP and SP measured by R3DR2 on ISS in the period October 24, 2014–January 11, 2016. Along them are shown solar proton fluxes measured in geostationary orbit with the device "Space Environment Monitor" (SEM) (URL: <http://goes.gsfc.nasa.gov/text/databook/section05.pdf>) on the GOES 15 satellite with energies more than 10 MeV (blue curve) and more 100 MeV (green curve). Low dose levels of several  $\mu\text{Gy d}^{-1}$  in the lower part of the figure are of secondary protons.

Nine maxima observed in the curve of average daily doses of SEP measured with the device R3DR2 well correlated with the measured with the device SEM flux of protons with energy greater than 10 MeV and 100 MeV on the GOES 15 satellite. The highest peak of nearly  $3000 \mu\text{Gy d}^{-1}$  on June 22, 2015 was not observed in the channel with data from GOES 15 with energy greater than 100 MeV. Our doses of June 22, 2015 [15] showed that if you hold a work of astronauts outside the ISS, they would receive more than 2.84 mGy extra dose for six hours and a half, which is identical to the average dose inside the ISS of 15 days [16].

## 5. "Liulin-ISS-2" engineering model operation

The operation of the "Liulin-ISS-2" instrument starts with two cable connection of the interface block with 5 A 28 V power line and simulator of the CAN interface running on external PC.

The "Liulin-ISS-2" instrument has to be switched ON by the ON/OFF tumbler on the right panel of IB. The green LED there indicates it. Then the tablet PC is switched ON by the right side green button (with a standard network switching symbol) on it (see Fig.1). This starts the loading of the Windows-8 OS

which lasts ~30 s. The "Liulin-ISS-2.exe" application is started automatically, which produce on the tablet PC screen an empty of information screenshot similar to that in Fig. 8. When you first turn ON the "Liulin-ISS-2" dosimeter on ISS the current time will be taken from the PC. After each connection with the CAN communication interface the time is updated with the on-board time automatically.



Fig. 8. Screenshot of empty of information "Liulin-ISS-2"

The internal dosimeter starts to measure with 10-s resolution the current background doses. When on earth their average values are in the range  $0.05 \div 0.2 \mu\text{Gy h}^{-1}$ , it is simply confirmed the measurements correctness. Each new measurement is displayed on the screen of tablet PC. After 90 minutes of measurements, which is about the time for 1 orbit on ISS, the curve with measured values, displayed on the screen of PC is similar to this seen in Fig. 9. Further the curve on the screen continue to be updated in a dynamical way, i.e. when new value is added at the right side the oldest value in the left side is removed. The values seen in the curve in Fig. 9 are between 0.03 and  $4 \mu\text{Sv h}^{-1}/\mu\text{Gy h}^{-1}$ . The average value is  $0.116 \mu\text{Sv h}^{-1}/\mu\text{Gy h}^{-1}$ . These values are normal for the background radiation [27].

The explanation of the tablet PC screenshot content is presented in Fig. 9. (All labels in the screenshot are in Russian. Alternative English language variant is developed also). The English language explanations are black printed around the screenshot. In the bottom of Fig. 9 in three white ovals the begin date/time, the elapsed time and the current time are displayed respectively. The second values are upgraded after each 10-s exposition time interval. In the third one the current time is running with 1-s resolution.

The measured dose rates in the last 10-s are shown in the oval in the upper left corner of the image. The left value of  $0.101 \mu\text{Gy h}^{-1}$ , situated in blue oval is the absorbed dose rate in the Silicon of the detector. This numeric value is represented graphically with the last seen in the left curve point. It is in  $\mu\text{Gy h}^{-1}$  and is calculated by the formula (1). The second value also of 0.101, situated in a red oval, is the calculated by formula (2) ambient dose equivalent dose rate in  $\mu\text{Sv h}^{-1}$ . We decide to use the GCR formula (2) because the conclusions from the "Dose

determination” section of the article says that the high LET part of the spectra is populated by protons, neutrons, and ions heavier than H<sup>+</sup>.

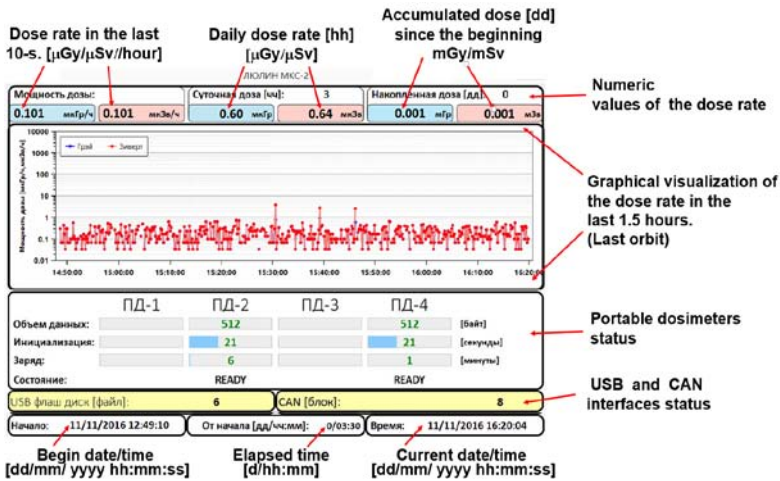


Fig. 9. Explanation of the tablet PC screenshot content

The absorbed dose rates are first plotted in the curve below by blue points and connected also by blue lines. Only 3 blue points are seen in the middle of the graphic. The reason is that the calculated by formula (2) ambient dose equivalent dose rate values in  $\mu\text{Sv h}^{-1}$  in the most of the natural background radiation measurements overlap the absorbed dose rate values, which leads that mostly red points and lines are seen in the curve. The ambient dose equivalent rate values are same as the absorbed dose rates because there aren't counts in the high LET part of the spectrum after 15<sup>th</sup> channel. Only in 3 measurements from about 540, sporadic particles from GCR origin are registered in some of the channels above number 15<sup>th</sup> and the calculated ambient dose rate red symbols are seen above the blue symbols of the absorbed dose rate in the curve.

The daily absorbed and ambient dose rates measured for 3 hours (3:30 hours precisely) are printed in the middle oval in the upper part of Fig. 9. The value of 0.6  $\mu\text{Gy}$  can be obtained by multiplication of the average dose rate of 0.116  $\mu\text{Gy h}^{-1}$  by 1890 measurements for 3 hours and 30 minutes divided by 360 to proceed from  $\mu\text{Gy h}^{-1}$  to  $\mu\text{Gy}$ . The daily ambient dose equivalent rate is a bit larger with a value of 0.64  $\mu\text{Sv}$ .

The total accumulated dose rates in mGy and mSv are shown in the oval in the right upper corner of the screenshot in Fig. 9. The two identical values of 0.001 mGy and mSv are the round off value of 0.6  $\mu\text{Gy}$  and 0.64  $\mu\text{Sv}$  to the upper value.

The two PD has to be connected to IB and switched ON. The PD battery charge starts. Then, the IB automatically reads and stores in the memory file the available data. The PD microcontroller informed IB when the battery is fully charged and this stops the process. The IB clears the PD memory and initiates them with: 1) the current date/time from PC, which is stored and upkeep in the PD clock-calendar; 2) the preselected exposition of 10-s or any other up to 1 h, required by the operator (cosmonaut). The PD has to be switched OFF and then disconnected from IB. After this it is ready to be used in places of interest inside or outside the ISS in a single or multiply sessions. Each new switching ON will produce a new file in the PD connected with the running in the PD clock-calendar. The maximum expected time of independent operation of PD is more than 7 days at 10-s resolution.

The “Portable dosimeters status” fields in Fig. 9 are divided in 4 columns, or one column for each possible PD. In the case of the "Liulin-ISS-2" engineering model only PD#2 and PD#4 are available. In the first row of each PD column the amount of the transmitted to the PC bytes is recorded and it is equal to 512 bytes for each PD. Next row shows that both PD has been initiated for 21 s each. The third row indicates how long in minutes the charging of the batteries up to the “Full charge” continued. Because both PD were almost fully charged the reported charging time is 6 minutes for PD#2 and 1 minute for PD#4. The last row indicates the status of the PD. It is “READY” for both of them, which confirms to the operator (cosmonaut) that each of them is ready to be used again. It has to be switched OFF and disconnected from the USB cable.

The “USB and CAN interfaces status” yellow ovals give information about: 1) how many files has been transmitted toward the removable USB stick. In this case the number of files are 6; 2) how many blocks has been transferred toward the CAN interface. In this case are they are 8.

In Fig. 10a is presented a simulation of a possible 1.5 h curve on ISS. The data from the R3DE instrument outside ISS [11] were obtained on 7 July 2009. Their full day absorbed dose rate curve in seen in Fig. 10b. For a better understanding of the data the brown line in Fig. 10b represents the variations of the ISS geographic latitude ( $\varphi$ ) between  $-51.6^\circ$  and  $51.6^\circ$ . The blue line meander of data with values between 0.03 and 20  $\mu\text{Gy h}^{-1}$  is from the GCR source, while higher value data up to 1570  $\mu\text{Gy h}^{-1}$  are from the IRB source. The 4 descending SAA maxima are first seen and second 4 ascending maxima. The simulated on the Fig. 10a data are highlighted with a green rectangle.

The English language screenshot is used in Fig. 10a. The meaning of the data in the ovals in the upper part of Fig 10a is same as already described. The horizontal axes is devoted to the universal time but in this case we use an accelerated in the time variant of the simulating software that is why the values there are not the correct UT values but the time of about 1-minute which represent the used by the software time for the simulation.



The curve represents first relatively low value data from the minimum, observed close to the geomagnetic equator. Next ISS moves to the high North hemisphere high latitudes where the GCR dose rates rise up. Two separate blue and red points and lines are clearly seen there. The blue points are calculated by formula (1), while the red points are calculated by formula (2). As these graphic data on the “Liulin-ISS-2” screen will be used only for visualization, for the separation of the GCR from the IRB data we use simple requirements: all data below  $20 \mu\text{Gy h}^{-1}$  are from the GCR source, while all data above are from the IRB source.

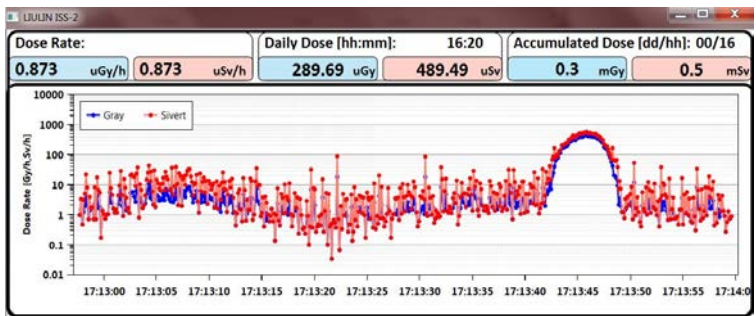


Fig. 10a. Simulation of the expected curve of measurements on ISS for 17 hours and 20 minutes. Real data from the R3DE instrument were used.

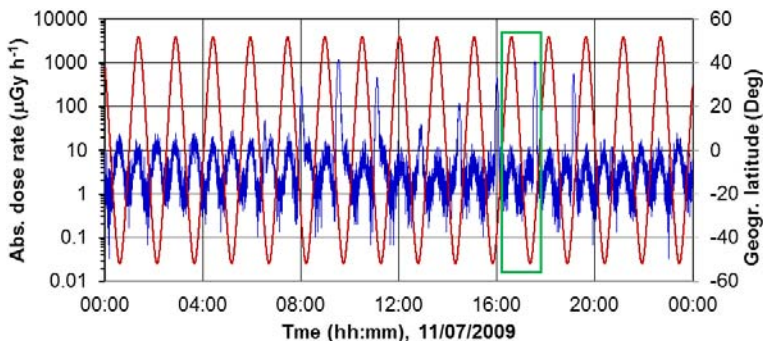


Fig. 10b. Real measured doses on 11 July 2009 by R3DE instrument on ISS

The low level data in the middle of Fig. 10a are from descending crossings of the geomagnetic equator. Next ISS transverses the South hemisphere high latitude region and reaches the SAA region. All data till this point was interpreted as a GCR source and were calculated using formula (2). Fast increase of the absorbed dose rates in the SAA region above  $20 \mu\text{Gy h}^{-1}$  switched the formula for calculation toward formula (3) and this is well seen in Fig 10a with relatively close absorbed and ambient equivalent dose rates.

## Conclusions

During the period 1989–2016 the Liulin type low mass, dimension and price instruments proved their ability to characterize the radiation environment at the ground, mountain peaks, aircraft, balloon, rocket, and spacecraft. We hope that the newly developed “Liulin-ISS-2” instrument will continue this tradition. If we will succeed to perform with portable dosimeter active measurements during real EVA on ISS this will give important and new information about the real doses from different radiation sources and their fast dynamics.

## Acknowledgements

The authors would like to thank: [V. Petrov](#), and [I. Chernykh](#) from IBP–RAS, Moscow, Russia for the long lasting and fruitful scientific cooperation since the development of the first LIULIN instrument in 1986; G. Horneck and G. Reitz from DLR, Institute of Aerospace Medicine, Germany, D.-P. Häder, M. Lebert, and M. Schuster from Department für Biology der Friedrich-Alexander-Universität, Germany for the leadership and cooperation in the experiments on ESA Foton-M2/M3 spacecraft and ISS; [F. Spurny](#), and O. Ploc from Nuclear Physics Institute, Czech Republic for work on the radiological interpretation of Liulin data and for the leadership in the use of Liulin instruments on aircraft; K. Fujitaka, Y. Uchihori, and H. Kitamura from National Institute of Radiological Sciences, Chiba, Japan for the leadership in the calibrations of Liulin instruments on protons and heavy ions; J. Lemaire from Institut d'Aeronomie Spatiale de Belgique for the help in the interpretation of LIULIN data; Gh. Gregoire and H. Schrnitz from Institut de Physique, Universite Catholique de Louvaln, Belgium, for the “Liulin-ISS” calibrations; E.G. Stassinopoulos, former Director of NASA-GSFC Radiation Physics Office, for the support in the “Liulin-3M” calibrations; E. Benton from Department of Physics, Oklahoma State University, USA for the support and NASA balloon data; J. Miller, Lawrence Berkeley National Laboratory, Berkeley, USA for the post-calibrations of LIULIN instrument; ISRO staff and specially to: M. Annadurai, Project Director and J.N. Goswami, Project scientist of Chandrayaan-1 satellite, P. Sreekumar and V. Sharan, Space Astronomy & Instrument Division, ISRO, Bangalore, India for the RADOM instrument support; M.T. Giardi and M. Damasso from Institute of Crystallography–National Research Council, Rome, Italy for the Liulin-Photo cooperation.

## References

1. Dachev, Ts. Analysis of the space radiation doses obtained simultaneously at 2 different locations outside ISS, *Adv. Space Res.*, 2013, 52, 1902–10. DOI: 10.1016/j.asr.2013.08.011

2. Benton, E.R., E.V. Benton, A.L. Frank, and M.F. Moyers. Characterization of the radiation shielding properties of US and Russian EVA suits using passive detectors, *Radiation Measurements*, 2006, 41, 1191–1201.
3. Dachev, T., B. Tomov, Y. Matviichuk, P. Dimitrov, G. De Angelis, Y. Uchihori, and O. Ploc. Main Specifications of New Liulin Type Intelligent Crew Personal Dosimeter, *Proceedings of 6<sup>th</sup> Scientific Conference with International Participation “Space, Ecology, Safety” SES’2010, Sofia, ISSN 1313-3888*, 76–82, 2011, URL: [http://www.space.bas.bg/SENS/SES2010/1\\_SpPh/10.pdf](http://www.space.bas.bg/SENS/SES2010/1_SpPh/10.pdf).
4. *Letter to the Editor* Ts.P. Dachev; N.G. Bankov; G. Horneck; D.-P. Häder. *Radiation Protection Dosimetry*, 2016. DOI: 10.1093/rpd/ncw123
5. Dachev, Ts.P., B. T. Tomov, Yu. N. Matviichuk, Pl. G. Dimitrov, N.G. Bankov, G. Horneck, and D.-P. Häder. Overview of the ISS radiation environment observed during EXPOSE-R2 mission in 2014-2016, *Space weather*, 2017. (Submitted)
6. ГОСТ 25645.203-83. Безопасность радиационная экипажа космического аппарата в космическом полете. Модель тела человека для расчета тканевой дозы. Госстандарт, Москва, 1984.
7. Мирошниченко, Л. И., Петров В. М. Динамика радиационных условий в космосе. М., Энергоатомиздат, 148 с., 1985.
8. ICRP Publication 60. Recommendations of the International Commission on Radiological Protection, 1990, Pergamon Press.
9. Dachev, Ts.P., Semkova J., Tomov B., Matviichuk Yu., Dimitrov Pl., Koleva R., Malchev St., Reitz G., Horneck G., Angelis G. De, Häder D.-P., Petrov V., Shurshakov V., Benthin V., Chernykh I., Drobyshev S., and Bankov N.G. Space Shuttle drops down the SAA doses on ISS. *Adv. Space Res.* 47, 2030–38, 2011, DOI: 10.1016/j.asr.2011.01.034
10. Dachev, Ts.P., B.T. Tomov, Yu.N. Matviichuk, P.G. Dimitrov, and N.G. Bankov. Relativistic Electrons High Doses at International Space Station and Foton M2/M3 Satellites. *Adv. Space Res.*, 44, 1433–40, 2009, DOI: 10.1016/j.asr.2009.09.023
11. Dachev, Ts., G. Horneck, D.-P. Häder, M. Lebert, P. Richter, M. Schuster, and R. Demets. Time profile of cosmic radiation exposure during the EXPOSE-E mission: the R3D instrument. *Astrobiology*, 2012, 12(5), 403–411. DOI: 10.1089/ast.2011.0759
12. Dachev, Ts., G. Horneck, and D.-P. Häder, M. Schuster, and M. Lebert. EXPOSE-R cosmic radiation time profile. *Astrobiology*, 2015, 14, 17–25. DOI: 10.1017/S1473550414000093
13. Shurshakov, V. A., V. M. Petrov, Yu.V. Ivanov, V. A. Bondarenko, V. V. Tzetlin, V. S. Makhmutov, Ts.P. Dachev, and J.V. Semkova. Solar particle events observed on MIR station, *Radiation Measurements*, 1999, 30, 317–325. DOI: 10.1016/S1350-4487(99)00058-X
14. Semkova, J., Ts. Dachev, R. Koleva, N. Bankov, S. Maltchev, V. Benthin, V. Shurshakov, and V. Petrov. Observation of radiation environment in the International Space Station in 2012–March 2013 by Liulin-5 particle telescope, *J. Space Weather Space Clim.* 2014, 4, A32. DOI: 10.1051/swsc/2014029

15. Dachev, Ts.P., B. T. Tomov, Yu. N. Matviichuk, Pl. G. Dimitrov, N.G. Bankov. High dose rates obtained outside ISS in June 2015 during SEP event, *Life Sciences in Space Research*, 2016, 9, 84–92. DOI: 10.1016/j.lssr.2016.03.004
16. Reitz, G., R. Beaujean, E. Benton, S. Burmeister, Ts. Dachev, S. Deme, M. Luszik-Bhadra, and P. Olko. Space radiation measurements on-board ISS—the DOSMAP experiment. *Radiat. Prot. Dosimetry*. 2005, 116, 374–379. DOI: 10.1093/rpd/nci262
17. Narici, L., M. Casolino, L. Di Fino, M. Larosa, P. Picozza, and V. Zaconté. Radiation survey in the International Space Station. *J. of Space Weather and Space Climate*. 2015, 5:A37, 14 p. DOI: 10.1051/swsc/2015037
18. Dachev, Ts.P., J.V. Semkova, B.T. Tomov, Yu.N. Matviichuk, Pl.G. S. Maltchev, R. Koleva, Pl., Dimitrov, N.G. Bankov, V.V., Shurshakov, V.V., Benghin, E.N., Yarmanova, O.A. Ivanova, D.-P. Häder, M.T. Schuster, G. Reitz, G. Horneck, Y. Uchihori, H. Kitamura, O. Ploc, J. Kubancak, and I. Nikolaev. Overview of the Liulin type instruments for space radiation measurement and their scientific results, *Life Sci. in Space Res.*, 2015, 4, 92–114. DOI: 10.1016/j.lssr.2015.01.005
19. Dachev, Ts.P. Characterization of near Earth radiation environment by Liulin type instruments. *Adv. Space Res.* 2009, 44, 1441–49. DOI: 10.1016/j.asr.2009.08.007
- 19a. Spurný, F., & Dachev, T. Long-term monitoring of the onboard aircraft exposure level with a Si-diode based spectrometer. *Advances in Space Research*, 2003, 32(1), 53–58. DOI: 10.1016/S0273-1177(03)90370-X
20. Dachev, Ts., B. Tomov, Yu. Matviichuk, Pl. Dimitrov, J. Lemaire, Gh. Gregoire, M. Cyamukungu, H. Schmitz, K. Fujitaka, Y. Uchihori, H. Kitamura, G. Reitz, R. Beaujean, V. Petrov, V. Shurshakov, V. Benghin, & F. Spurny. Calibration Results Obtained With Liulin-4 Type Dosimeters. *Adv. Space Res.* 2002, 30(4), 917–925. DOI: 10.1016/S0273-1177(02)00411-8
21. Spurny, F. Response of a Si-diode-based device to fast neutrons, *Radiation Measurements*, 2005, 39, 219–223. DOI: 10.1016/j.radmeas.2004.05.006
22. Ploc, O., F. Spurny, and Ts.P. Dachev. Use of Energy Depositing Spectrometer for Individual Monitoring of Aircrew, *Radiat. Prot. Dosimetry*, 2011, 144(1–4), 611–614. DOI: 10.1093/rpd/ncq505
23. Green, A.R., L.G.I. Bennett, B.J. Lewis, F. Kitching, and M.J. McCall. Desormeaux, M., Butler, A., An empirical approach to the measurement of the cosmic radiation field at jet aircraft altitudes, *Adv. in Space Res.*, 2005, 36, 1618–26.
24. Spurny, F., O. Ploc, and I. Jadrníčková. Spectrometry of linear energy transfer and dosimetry measurements onboard spacecrafts and aircrafts. *Phys. Part. Nuclei Lett.*, 2009, 6, 70–77. DOI: 10.1134/S1547477109010117
25. Zhang, L., R. Mao, and R. Zhu. Fast neutron induced nuclear counter effect in Hamamatsu silicon PIN diodes and APDs, *IEEE Transactions on Nuclear Science*, 2011, 58(3), 1249–56. DOI: 10.1109/TNS.2011.2132144
26. Heffner, J. Nuclear radiation and safety in space. M, Atomizdat, 115 p., 1971. (In Russian).
27. Ghiassi-nejad, M., S.M.J. Mortazavi, J.R. Cameron, A. Niroomand-rad, and P.A. Karam. Very High Background Radiation Areas of Ramsar. 82. Preliminary Biological Studies. *Health Physics, Iran*, 2002, 87–93. URL: <http://www.probeinternational.org/Ramsar.pdf>.

## **ОПИСАНИЕ НА СИСТЕМАТА "ЛЮЛИН-МКС-2" ЗА ДОЗИМЕТРИЧЕН КОНТРОЛ НА КОСМОНАВТИТЕ В РАДИАЦИОННАТА СРЕДА НА МКС**

*Цв. Дачев, Б. Томов, Ю. Матвийчук, Пл. Димитров,  
В. Шуриаков, В. Бенгин, Е. Ярманова, О. Иванова, И. Николаев*

### **Резюме**

По договор между Института за космически изследвания към БАН, Института за био-медицински проблеми на РАН и Ракетно-космическа корпорация „Енергия“ е разработен инженерен модел на новата система за персонален дозиметричен контрол на руските космонавти в и извън Международната космическа станция (МКС) – „Люлин-МКС-2“. Очаква се новата система да замени системата „Люлин-МКС-1“ и да се фокусира върху активен мониторинг, с разрешение от 10 s на динамиката на мощността на дозата от галактически космически лъчи (ГКЛ), протони от вътрешния и енергийни електрони от външния радиационни пояси, и слънчеви енергийни частици (СЕЧ) в модулите на МКС и по време на активности извън станцията (АИС) на руски и международни космонавти. Значимостта на измерването на дозата по време на АИС е оценена при анализа на големи и бързи колебания в пространствено-времеви разпределения на дозите, получени едновременно на две различни места извън МКС. Инженерният модел на системата „Люлин-МКС-2“ се състои от 2 преносими дозиметри (ПД) и интерфейс блок (ИБ) с вътрешен дозиметър. ПД е с размери 66×56×26 mm и е продължение на традиционните дозиметри от типа „Люлин“ с един 1 PIN диод. Анализът на спектрите от дозиметрите ще се извършва съгласно идеите за интелигентен личен дозиметър на екипажа и новия опит, получен по време на анализа на данните от инструмента R3DR2 извън МКС в периода октомври 2014–януари 2016 г. Призматичната литиево-йонна акумулаторна батерия на фирмата SAFT, одобрена за използване в космическото пространство се използва в ПД и позволява повече от 7 дни самостоятелна работа с разрешение от 10 s. По време на АИС, когато ПД се намира в джоба на скафандъра на космонавта, за да се поддържа температурата на PIN-диода не по-малка от -20°C в ПД се използват термостат и управляем нагревател. ПД може да работи независимо от ИБ посредством USB интерфейс и специален софтуер, с който и да е друг компютър. Интерфейсният блок се управлява от таблетен персонален компютър (ПК) на фирмата Getac от типа T800. Той е изпълнен в съответствие с изискванията и процедурите на стандарта MIL-STD-810G и е под ОС Windows-8. ПК управлява системата чрез 8-портов USB хъб, който свързва ПК с дозиметрите, CAN-интерфейса и външната флаш памет. Данните, получени с вътрешния дозиметър, за последната орбита (~90 минути) се визуализират непрекъснато на екрана на компютъра и ще бъдат използвани от космонавтите и наземния радиационен контрол за бърза оценка на риска за здравето на космонавтите по време на слънчеви протонни събития.